AD-A179 491 GRADED BANDGAP SOLAR CELLS(U) WASHINGTON UNIV RICHLAND 1/1
JOINT CENTER FOR GRADUATE STUDY L C OLSEN 01 SEP 84
AFOSR-TR-87-0493 AFOSR-84-0355

UNCLASSIFIED F/G 10/2 NL

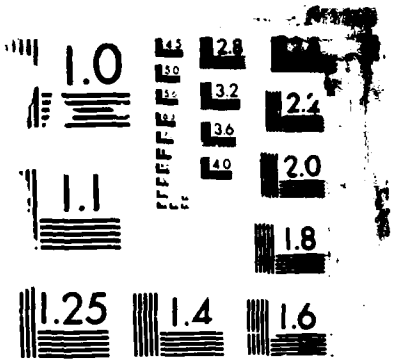
1.0
1.1
1.25
1.4
1.6
1.8
2.0
2.2
2.8
3.2
3.6
4.0

(2)

DTIC FILE COPY

AD-A179 491

AFOSR-TR- 87-0493

GRADED BANDGAP SOLAR CELLS

Approved for public release;
[illegible] unlimited.

DTIC
ELECTE
APR 23 1987
S D
D

Annual Report

for period

9/1/85 - 8/31/86

AIR FORCE OFFICE OF SCIENTIFIC RESEARCH (AFSC)
NOTICE OF TRANSMITTAL TO DTIC
This technical report has been reviewed and is approved for public release IAW AFR 190-12.
Distribution is unlimited.
MATTHEW J. KERPER
Chief, Technical Information Division

AFOSR GRANT: AFOSR-84-0355

START DATE: 9/1/84

CONTRACTOR: University of Washington (Tri-Cities University Center)

PRINCIPAL INVESTIGATOR: Dr. Larry C. Olsen

DISTRIBUTION STATEMENT A
Approved for public release;
Distribution Unlimited

LEX96/2

87 4 21 134

UNCLASSIFIED

SECURITY CLASSIFICATION OF THIS PAGE

REPORT DOCUMENTATION PAGE

1a. REPORT SECURITY CLASSIFICATION Unclassified	1b. RESTRICTIVE MARKINGS AD-A179 491
2a. SECURITY CLASSIFICATION AUTHORITY	3. DISTRIBUTION/AVAILABILITY OF REPORT Approved for public release, distribution unlimited
2b. DECLASSIFICATION/DOWNGRADING SCHEDULE	
4. PERFORMING ORGANIZATION REPORT NUMBER(S)	5. MONITORING ORGANIZATION REPORT NUMBER(S) AFOSR-TR- 87-0493
6a. NAME OF PERFORMING ORGANIZATION University of Washington Joint Center for Graduate Study	6b. OFFICE SYMBOL (If applicable)
6c. ADDRESS (City, State and ZIP Code) 100 Sprout Road Richland, Washington 99352	7a. NAME OF MONITORING ORGANIZATION AFOSR
	7b. ADDRESS (City, State and ZIP Code) same as 8c.
8a. NAME OF FUNDING/SPONSORING ORGANIZATION AFOSR	8b. OFFICE SYMBOL (If applicable) NP
	9. PROCUREMENT INSTRUMENT IDENTIFICATION NUMBER AFOSR-84-0355
8c. ADDRESS (City, State and ZIP Code) Building 410 Bolling AFB, D.C 20332-6448	10. SOURCE OF FUNDING NOS. PROGRAM ELEMENT NO. 61102F; PROJECT NO. 2301; TASK NO. A7; WORK UNIT NO.
11. TITLE (Include Security Classification) "GRADED BANDGAP SOLAR CELLS" (U)	
12. PERSONAL AUTHOR(S) Dr. Olsen	
13a. TYPE OF REPORT ANNUAL	13b. TIME COVERED FROM 85/09/01 TO 86/08/31
14. DATE OF REPORT (Yr., Mo., Day)	15. PAGE COUNT 32
16. SUPPLEMENTARY NOTATION	

17 COSATI CODES		
FIELD	GROUP	SUB. GR.

18. SUBJECT TERMS (Continue on reverse if necessary and identify by block number)
Solar Cells, Graded Bandgap, Space Power

19. ABSTRACT (Continue on reverse if necessary and identify by block number)

Graded bandgap solar cells were investigated that have a structure consisting of an N-type graded emitter and a base region with a constant bandgap. The emitter bandgap was 2.1 eV at the front surface and then graded to 1.74 eV at the N/P homojunction based on a 1.74 eV bandgap. The AlGaAs homojunction had a maxium value for internal photoresponse of 20% while the graded bandgap cell exhibited a peak value of 80%. Analyses of photoresponse data indicates the AlGaAs homojunctions are characterized by minority carrier diffusion lengths of only .03um in the emitter and 0.1 um in the base. Thus, the effective field resulting from the graded emitter in the graded bandgap cell is necessary for an adequate photoresponse. Investigations of heteroface GaAs solar cells continued with the purpose of building a data base for processing technology and characterization techniques. GaAs solar cells were fabricated with efficiencies over 17% using a P/N homojunction structure ans AlGaAs heteroface. Electro-optical characterization of GaAs cells has resulted in improved understanding of minority carrier properties, surface recombination velocity and current loss mechanisms.

20. DISTRIBUTION/AVAILABILITY OF ABSTRACT UNCLASSIFIED/UNLIMITED ☐ SAME AS RPT. ☒ DTIC USERS ☐	21 ABSTRACT SECURITY CLASSIFICATION UNCLASSIFIED
22a. NAME OF RESPONSIBLE INDIVIDUAL BRUCE L. SMITH	22b TELEPHONE NUMBER (Include Area Code) (202)767-4907
	22c OFFICE SYMBOL NP

DD FORM 1473, 83 APR EDITION OF 1 JAN 73 IS OBSOLETE.

UNCLASSIFIED

SECURITY CLASSIFICATION OF THIS PAGE

TABLE OF CONTENTS

ABSTRACT

Graded bandgap solar cells were investigated that have a structure consisting of an N-type graded emitter and a base region with a constant bandgap. The emitter bandgap was 2.1 eV at the front surface and then graded to 1.74 eV at the N/P junction. The device exhibited an enhanced photoresponse compared to a N/P homojunction based on a 1.74 eV bandgap. The AlGaAs homojunction had a maximum value for internal photoresponse of 20%, while the graded bandgap cell exhibited a peak value of 80%. Analyses of photoresponse data indicates the AlGaAs homojunctions are characterized by minority carrier diffusion lengths of only .03 μm in the emitter and 0.1 μm in the base. Thus, the effective field resulting from the graded emitter in the graded bandgap cell is necessary for an adequate photoresponse. Investigations of heteroface GaAs solar cells continued with the purpose of building a data base for processing technology and characterization techniques. GaAs solar cells were fabricated with efficiencies over 17% using a P/N homojunction structure and AlGaAs heteroface. Electro-optical characterization of GaAs cells has resulted in improved understanding of minority carrier properties, surface recombination velocity and current loss mechanisms.

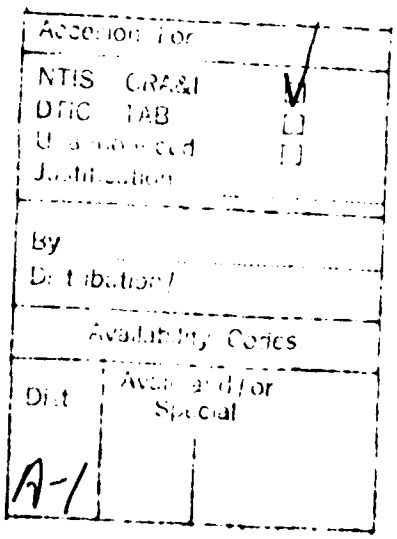

1. INTRODUCTION AND SUMMMARY

One of the approaches being pursued for fabricating high efficiency solar cells involves the use of two or more cells having different bandgaps. By utilizing more than one bandgap, a photovoltaic system can be coupled to the solar spectrum in a more optimum manner than that achieved with a single homojunction cell. The most common approach to constructing a multiple cell system involves arranging devices in tandem, in order of the bandgaps, and with largest bandgap cell receiving the incident photons.

Tandem cell systems can be constructed in two ways: by growing a monolithic stack, or by arranging the devices in a mechanical stack. With either approach, system efficiencies of 30% are considered reasonable goals. In order to obtain efficiencies of 50%, a stack of three to five cells will be required. Even if film growth technology is developed that allows the formation of a five-cell stack, it will be difficult to form the interconnecting regions without creating regions of high electron-hole recombination, or regions of high photon absorption.

An alternative cell structure which has a large limiting efficiency is that of a graded bandgap solar cell. The graded bandgap cell is designed to produce a large photocurrent at a relatively large voltage. The device involves only one N-type to P-type transition, and is therefore only a two-terminal cell.

1.1 Graded Bandgap Cell Concept

The basic approach of interest in this program is depicted in Figure 1. The front surface is P-type and has a large bandgap, E_{gmax}. The bandgap in the emitter region is gradually reduced to E_{gmin} at which point a junction is formed with a large bandgap N-type region. Clearly, the order of the P- and N-type materials can be reversed. Ideally, the variation in E_g vs. x is chosen so that the system will operate as a 'black' cell, so that J_{sc} can approach the maximum value. For example, if E_g is varied properly, then photons with energy $h\nu_2$ will penetrate to only an infinitesimal depth past $x = x_2$, thus minimizing the energy lost to the lattice.

INCREASED PHOTOCURRENT

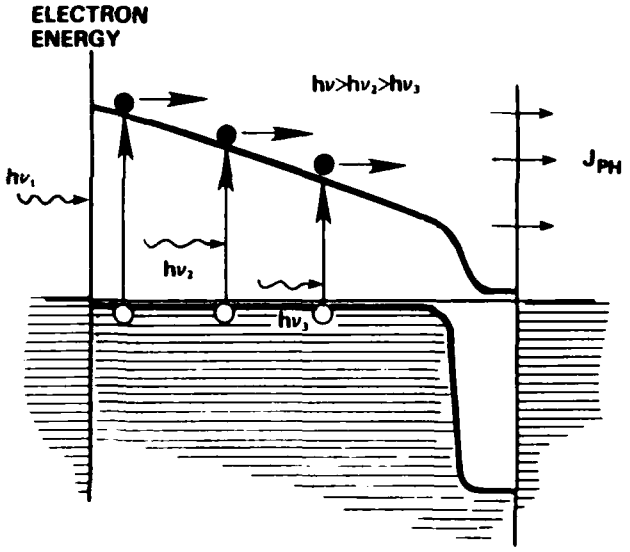

- GRADE BANDGAP TO OPTIMIZE COUPLING BETWEEN SOLAR SPECTRUM AND CELL PHOTORESPONSE
- PHOTOCURRENT CAN APPROACH THE MAXIMUM VALUE.

INCREASED VOLTAGE

(MINIMUM CARRIER RECOMBINATION)

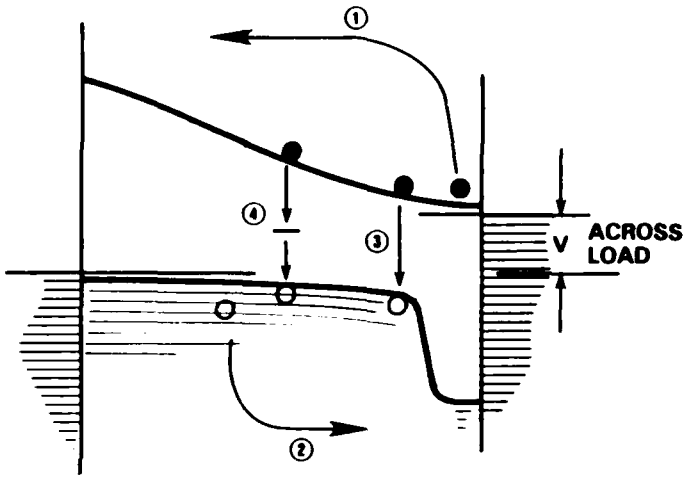

- THERMALLY ACTIVATED LOSS CURRENTS ① AND ② ARE NEGLIGIBLE BECAUSE OF LARGE BANDGAPS AT END FACES
- BAND-TO-BAND RECOMBINATION ③ REDUCED BY MINIMIZING LOW BAND GAP REGION
- RECOMBINATION VIA DEFECT ENERGY LEVELS ④ MINIMIZED BY GRADING MATERIAL COMPOSITION SUCH THAT LATTICE CONSTANT REMAINS THE SAME

Figure 1. Graded Bandgap Solar Cells: Physical Principles Under Investigation.

Graded bandgap cells have the potential for exhibiting large values of both photocurrent and open circuit voltage. Assuming the availability of a materials system with which one can vary the bandgap continuously over the energy range appropriate for the solar spectrum, and assuming the bandgap always to be direct in nature, the graded bandgap structure will allow one to obtain maximum photocurrent. Assuming no concentration, the maximum possible photocurrent value will approach 50 mA/cm^2 under AM1 conditions. The open-circuit voltage, and also the maximum power developed by the cell will be dictated by the current loss mechanisms--or electron-hole recombination mechanisms. Referring to Figure 1, it is expected that devices fabricated in the near term will exhibit current-voltage characteristics determined by mechanisms No. 3 and No. 4. As material is obtained with longer and longer minority carrier lifetimes, current losses could eventually be dominated by mechanisms No. 1 and No. 2, thermionic emission over the barriers at the two end faces.

If we assume that the bandgap of the two end faces is 2.5 eV, then one can estimate that the limiting value for the reverse saturation current (J_o) would be on the order of 10^{-35} A/cm^2. Assuming J_{sc} = 50 mA/cm^2, the AM1 efficiency is calculated to be significantly larger than 50%.

J_o-values on the order of 10^{-35} A/cm^2 are very unlikely to be achieved. However, J_o-values less than of 10^{-19} A/cm^2 have been achieved for GaAs devices. If one assumes J_{sc} = 50 mA/cm^2 and $J_o = 10^{-19}$ A/cm^2, the AM1 efficiency is determined to be 48%. Thus, efficiencies on the order of 50% are possible for graded bandgap cells. As a result, the graded bandgap cell is worthy of investigation.

1.2 Research Objectives

The overall objective of this program is to investigate the feasibility of achieving high efficiencies with graded bandgap solar cell structures. Specific objectives include: (1) fabricate graded bandgap cells based on the $Al_xGa_{1-x}As$ ternary compound system; (2) measure electro-optical properties of the devices and interpret results in terms of appropriate models; and (3) develop approaches to modeling calculations for graded bandgap cells.

1.3 Technical Approach

Figure 2 summarizes some of the key elements of the technical approach being taken in this program. Graded bandgap solar cell structures are being investigated by fabricating and characterizing devices based on the $Al_xGa_{1-x}As$ materials system. As x is varied from x = 0 (GaAs) to x = 1.0 (AlAs), the bandgap changes from 1.42 eV to 2.18 eV, respectively. Throughout this composition range, the change in lattice constant is less than 1%. As a result, graded regions can be grown without the generation of misfit dislocations.

The $Al_xGa_{1-x}As$ compounds are characterized by a direct bandgap for x-values between x = 0 (E_g = 1.42 eV) and x = 0.45 (E_g = 1.96 eV). Thus, these materials are efficient optical absorbers as required for a graded solar cell. Another benefit of using the $Al_xGa_{1-x}As$ materials system for these studies is that the materials technology is relatively advanced. Multilayered structures based on the AlGaAs system can be grown by metal organic chemical vapor deposition (MOCVD). Growth of AlGaAs by MOCVD can be purchased as a service by several industrial companies. We will be obtaining a MOCVD system during the summer of 1987 as a result of a DoD equipment grant. Thus, these structures can eventually be grown in-house.

The technical approach to this program involves three key activities: (1) fabrication of graded AlGaAs solar cells and GaAs heteroface solar cells; (2) electro-optical and physical characterization of solar cells; and (3) modeling calculations to assist in device design and interpretation of performance data.

1.4 Status of Research

Efforts in FY86 concentrated on fabrication and characterization of graded AlGaAs solar cells and heteroface GaAs solar cells. Graded solar cells were fabricated based on a graded N-type emitter involving the bandgap changing from 2.18 eV (x = 0.9) to 1.74 eV (x = 0.25) at the junction, and a P-type base region with E_g = 1.74 eV. AlGaAs homojunction cells were also fabricated based on a N/P structure and E_g = 1.74 eV (x = 0.25). Photoresponse measurements taken for the AlGaAs graded cell and homojunction clearly show the effects of the effective field of the graded emitter. Studies of graded

MATERIAL SYSTEM

- III-V COMPOUNDS
- EFFICIENT OPTICAL ABSORBERS
- ADVANCED MATERIALS TECHNOLOGY

DEVICE FABRICATION

- THIN FILM DEVICE STRUCTURES BEING FABRICATED BY METAL ORGANIC CHEMICAL VAPOR DEPOSITION.
- CONTACTS AND ANTI-REFLECTION COATINGS APPLIED BY VACUUM DEPOSITION.

DEVICE CHARACTERIZATION

- CURRENT-VOLTAGE CHARACTERISTICS, PHOTORESPONSE, DEEP LEVEL SPECTROSCOPY AND OTHER DIAGNOSTIC MEASUREMENTS ARE CONDUCTED ON CELLS.
- ELECTRO-OPITCAL CHARACTERISTICS INTERPRETED IN TERMS OF THEORY.

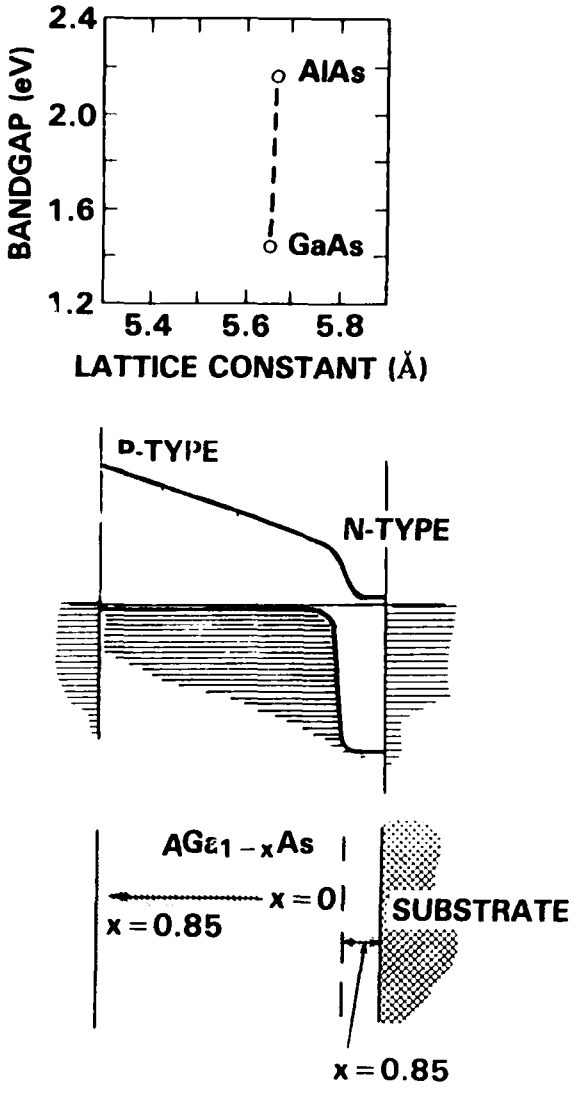

Figure 2. Graded Bandgap Solar Cells: Experimental Approach.

emitter structures are continuing. More optimized graded AlGaAs cells will be fabricated and are expected to exhibit significant improvements in efficiency relative to the corresponding AlGaAs homojunction.

GaAs P/N solar cells were also fabricated. The devices are investigated to develop a data base for contacting technology, to allow a comparison with other high efficiency GaAs cell results, and to establish current transport models for a simpler device structure than graded structures. GaAs solar cells with AlGaAs window layers were fabricated which exhibit an efficiency greater than 17%.

2. GRADED AlGaAs SOLAR CELLS

2.1 Cell Design and Fabrication

In order to study the effect of a graded bandgap emitter, two cell structures were fabricated, an AlGaAs homojunction, and a similar cell except that the emitter composition was graded. The electron band diagrams for the two devices are depicted in Figure 3. Other details such as dopant concentrations, layer thicknesses and layer composition are given in Tables 1 and 2. N-type emitters were used so that an adequate sheet conductance could be obtained.

2.2 Photoresponse of AlGaAs Cells

Internal photoresponse data shown in Figure 4 for the two types of AlGaAs cells illustrate in a rather dramatic fashion the effect of a graded bandgap emitter. The quantum efficiency of the graded emitter cell is greater than that of the homojunction cell by a factor of four. Analysis of the homojunction photoresponse revealed that the minority carrier diffusion lengths in both the N-type emitter and P-type base are very short. Thus, a graded emitter appears necessary for a cell based on $Al_xGa_{1-x}As$ with $x \simeq 0.25$.

Computer aided analyses of the homojunction photoresponse data were carried out. Figure 5 shows the best fit to the experimental data. The parameters corresponding to the best fit are:

$$\left[\begin{array}{l}\text{Surface Recombination}\\ \text{Velocity of the}\\ \text{Front Surface, S(F)}\end{array}\right] > 10^4 \text{ cm/sec}$$

$$\left[\begin{array}{l}\text{Surface Recombination}\\ \text{Velocity of the}\\ \text{Back Surface, S(B)}\end{array}\right] > 10^4 \text{ cm/sec}$$

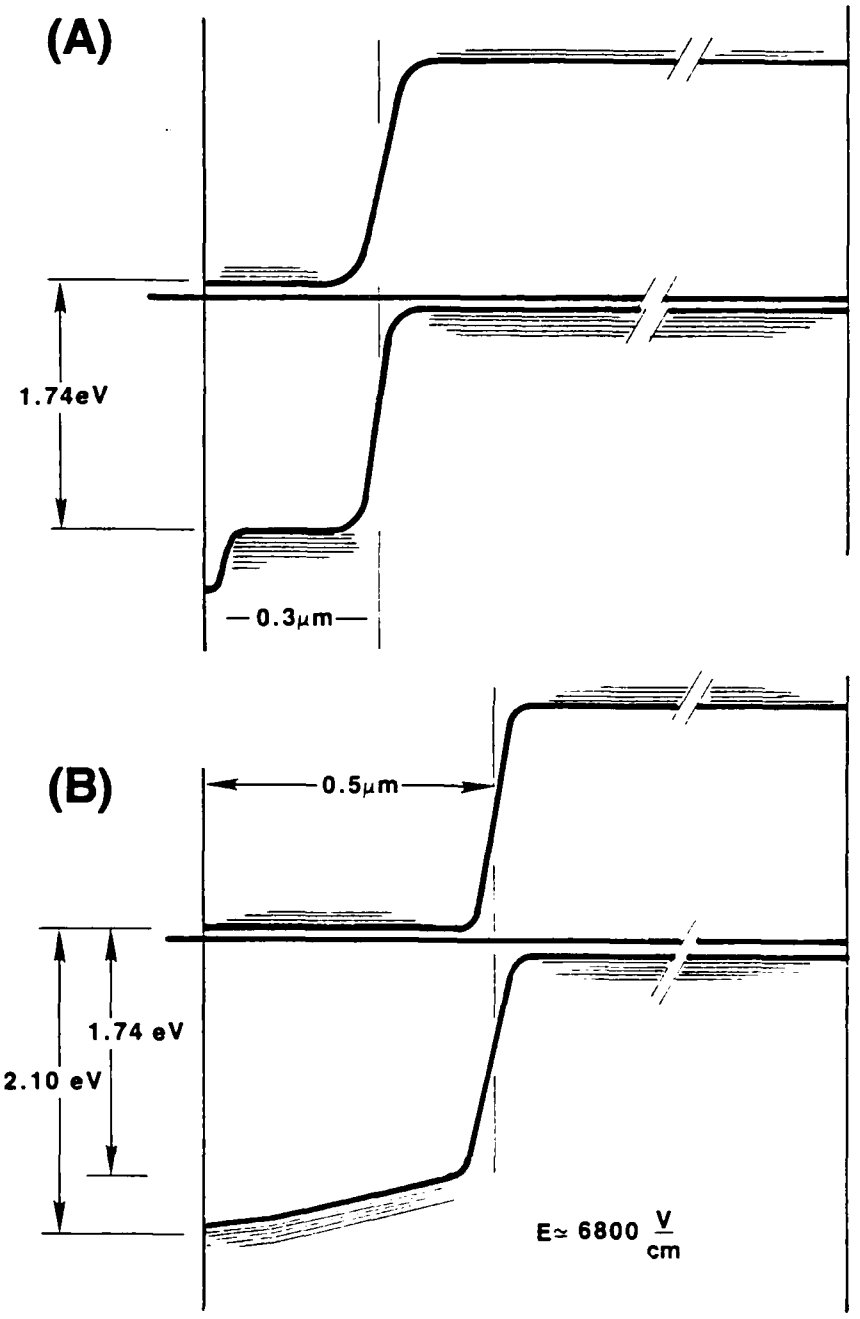

Figure 3. Electron Band Diagram for (A) AlGaAs Homojunction and (B) AlGaAs Graded Emitter Solar Cell.

Table 1

SPECIFICATIONS FOR GRADED AlGaAs HOMOJUNCTION SOLAR CELL

LAYER NUMBER	LAYER DESCRIPTION	DOPANT CONCENTRATION (cm^{-3})	LAYER THICKNESS (μm)
6	N^+-GaAs (Cap)	1×10^{18}	0.1
5	N-$Al_{.90}Ga_{.10}As$	$1\text{-}2 \times 10^{18}$	.05
4	N-$Al_{.25}Ga_{.75}As$	$1\text{-}2 \times 10^{18}$	0.3
3	P-$Al_{.25}Ga_{.75}As$	$1\text{-}2 \times 10^{18}$	3.0
2	P-$Al_{.90}Ga_{.10}As$	$1\text{-}2 \times 10^{18}$	0.1
1	P-GaAs (BUFFER LAYER)	$1\text{-}2 \times 10^{18}$	1.0
SUBSTRATE	P^+GaAs (CLASS A SUMITOMA)	$> 10^{18}$	

Table 2

SPECIFICATIONS FOR GRADED AlGaAs SOLAR CELL

LAYER NUMBER	LAYER DESCRIPTION	DOPANT CONCENTRATION (cm^{-3})	LAYER THICKNESS (μm)
5	N^+-GaAs (CAP)	$> 1 \times 10^{18}$	0.1
4 (GRADED)	N-$Al_{.90}Ga_{.10}As$ | N-$Al_{.25}Ga_{.75}As$	$1\text{-}2 \times 10^{18}$	0.5
3	P-$Al_{.25}Ga_{.75}As$	$1\text{-}2 \times 10^{18}$	3.0
2	P-$Al_{.90}Ga_{.10}As$	$1\text{-}2 \times 10^{18}$	0.1
1	P-GaAs (BUFFER LAYER)	$1\text{-}2 \times 10^{18}$	1.0
SUBSTRATE	P^+GaAs (CLASS A SUMITOMA)	$> 10^{18}$	

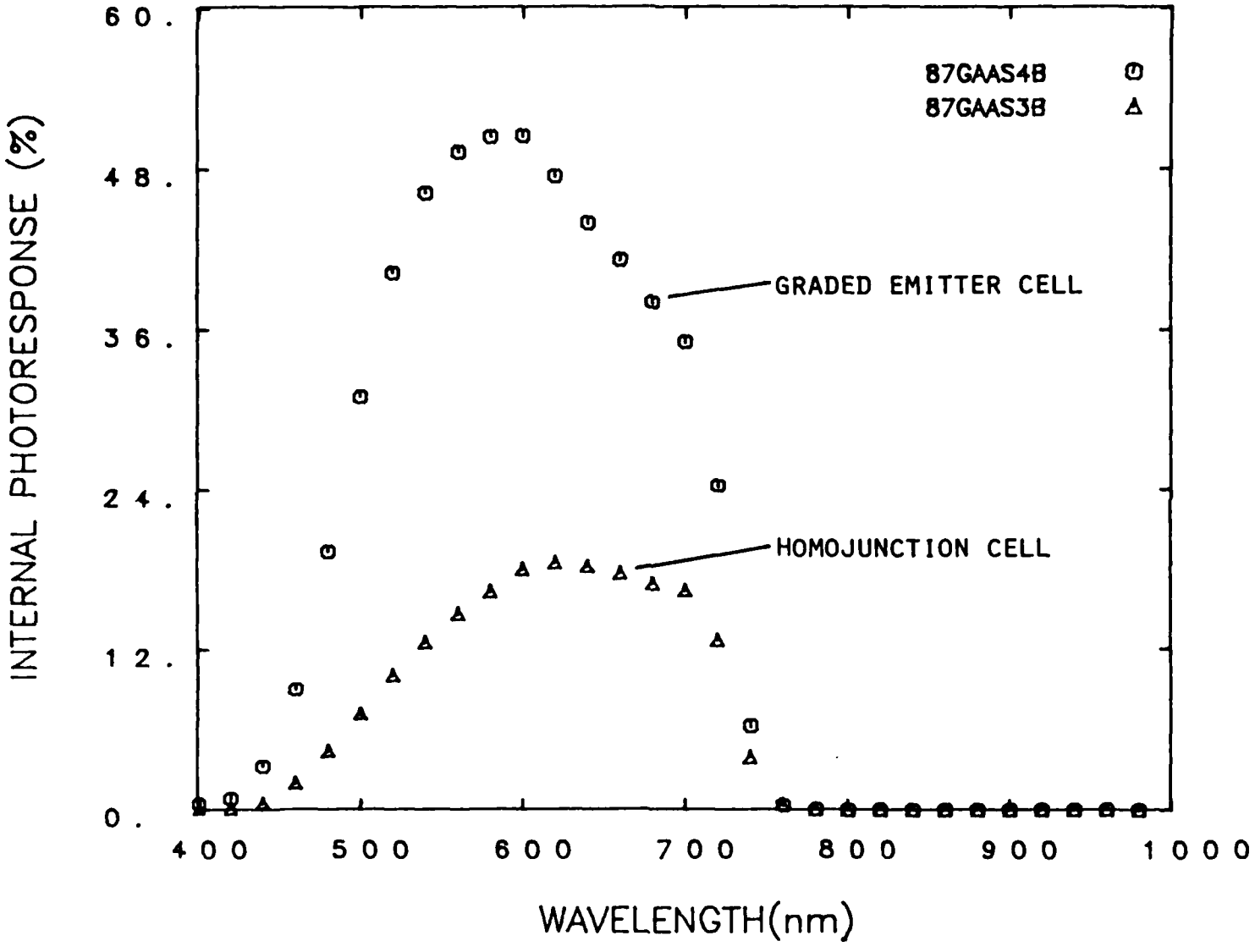

Figure 4. Internal Photoresponse Determined for AlGaAs Graded Emitter and Homojunction Solar Cells.

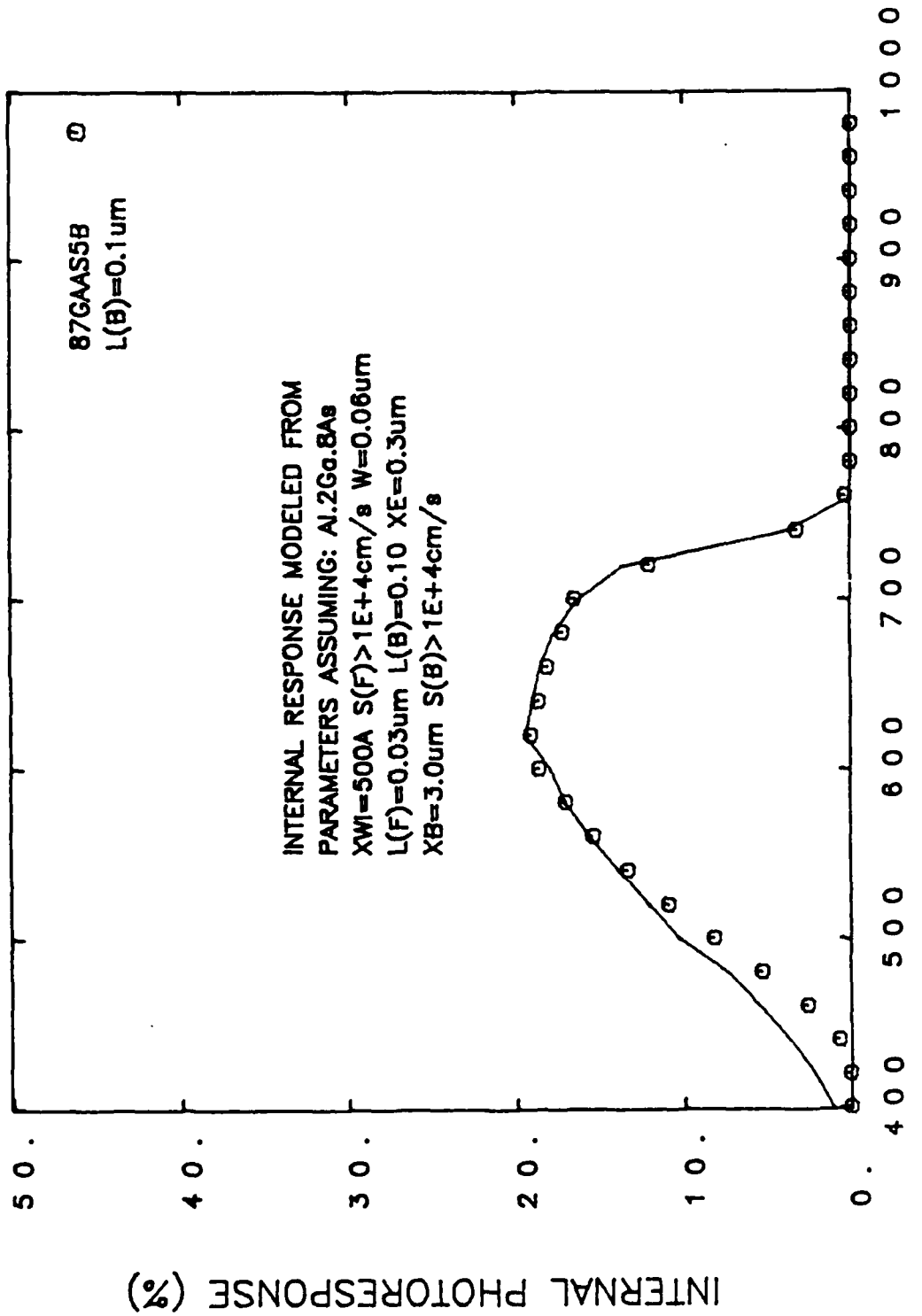

Figure 5. Internal Photoresponse Data and Theoretical Fit of Data for AlGaAs Homojunction Solar Cell.

Minority Carrier Diffusion Length for Emitter, L(F)	=	0.03 μm
Minority Carrier Diffusion Length for Base, L(B)	=	0.10 μm

The key results are the values obtained for L(F) and L(B).

The emitter diffusion length is very close to zero. If one assumes that L(F) and L(B) have similar values in the graded emitter cell, it is clear that the large difference in the photoresponse values is due to enhanced emitter collection that results from the effective built-in electric field.

The value obtained for L(B) is surprisingly low. These layered structures were grown by Epitronics. It appears that the $Al_xGa_{1-x}As$ layers are very defective. Larger diffusion lengths have been measured for P-type AlGaAs layers by researchers at Varian. However, it is generally assumed that N-type AlGaAs layers are characterized by low diffusion lengths.

3. GaAs HETEROFACE SOLAR CELLS

GaAs solar cells have been investigated in parallel with graded bandgap AlGaAs cells in order that baseline fabriction and characterization procedures can be established with a relatively familiar cell structure. In particular, metallization processes, AR layer deposition techniques, and modeling calculation procedures have been developed for GaAs solar cells. This technology information base can then be applied to graded bandgap structures.

3.1 Cell Fabrication and Performance

Solar cell structures studied are described by Figure 6. MOCVD film structures were grown according to specifications by industrial suppliers. Metallization, cap removal, and AR layer deposition are done at the Center. SiN_x deposited by plasma-enhanced CVD (PECVD) is utilized as a single AR coating. AM1 efficiencies in the range of 17% to 18% have been achieved with cells fabricated as discussed. Cells are typically 1.5 cm x 1.5 cm.

Figure 7 shows current-voltage characteristics for a P/N cell subjected to simulated AM1 illumination. The short-circuit current density will be increased significantly with a more optimized heteroface. Photoresponse studies indicate that the AlGaAs/GaAs interface is quite defective resulting in poor blue response and reduced J_{SC}. The open-circuit voltage (V_{OC}) will be increased as a result of increased J_{SC}, and also as a result of reduced current losses due to space charge recombination.

3.2 Photoresponse Studies

Spectral photoresponse studies are used to determine values for the front surface recombination velocity, S(F), the emitter minority carrier diffusion length, L(F), and the base minority carrier diffusion length, L(B). Experimental data are fit with theoretical expressions for photoresponse by varying these four parameters and accounting for photon absorption in the various layers of the device. Computer codes which calculate photon absorption, reflection and transmission in multilayer systems are utilized in the computer aided analyses. Some of the required optical absorption data are shown in Figure 8, namely, the optical absorption coefficient for $Al_xGa_{1-x}As$ for various values of x.

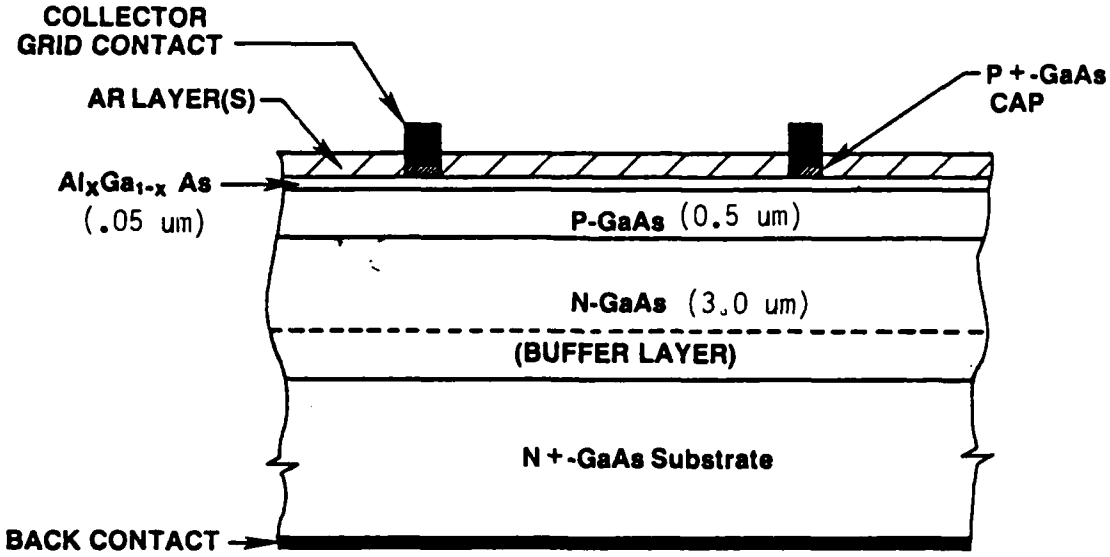

Figure 6. GaAs Solar Cell Structure.

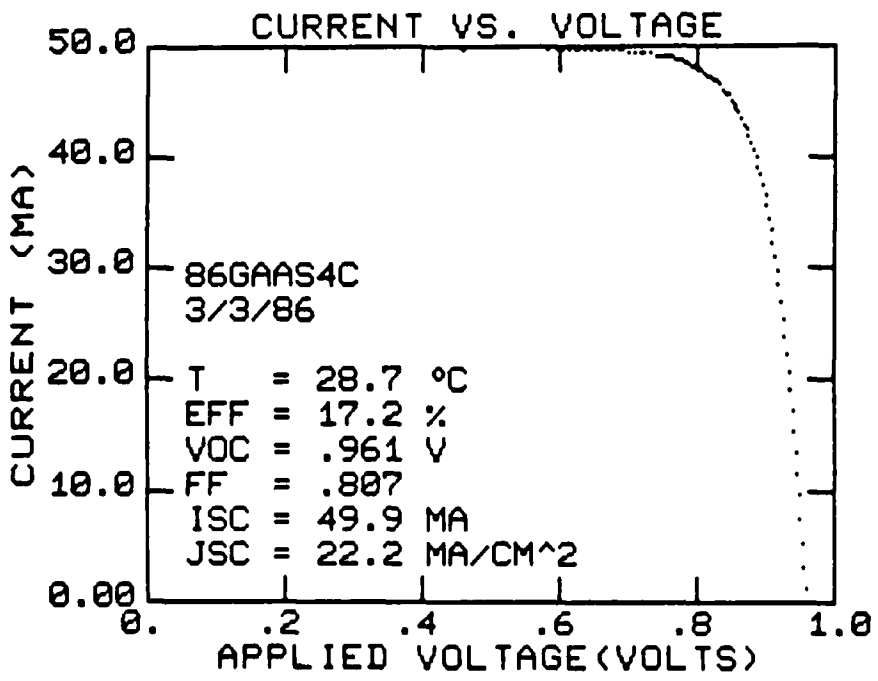

Figure 7. Illuminated Characteristics of GaAs P/N Solar Cell.

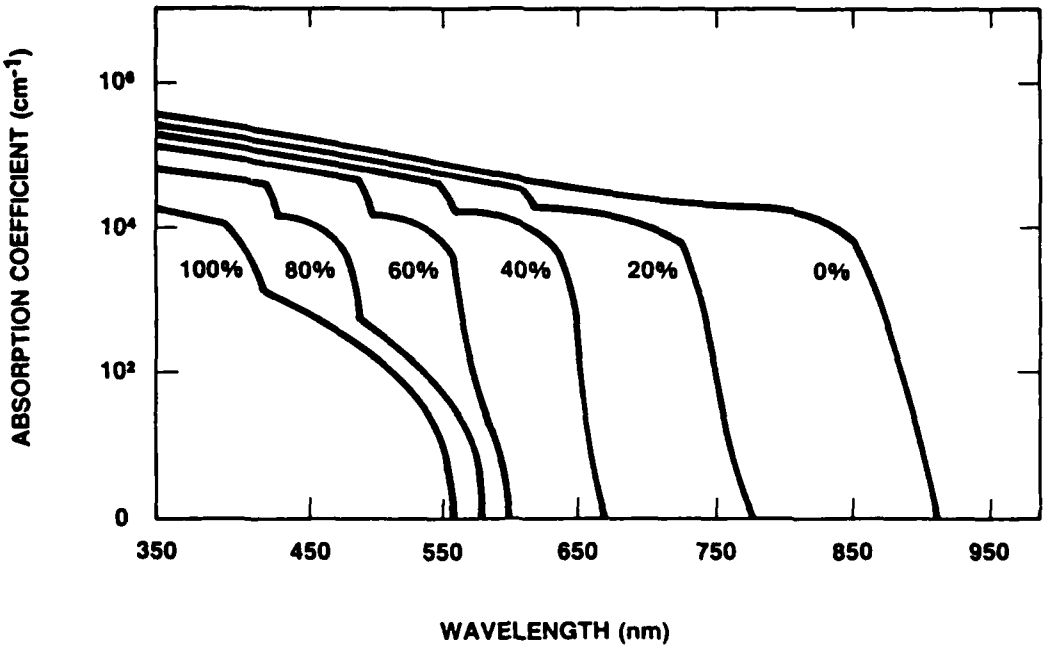

Figure 8. Absorption Coefficient for $Al_xGa_{1-x}As$.

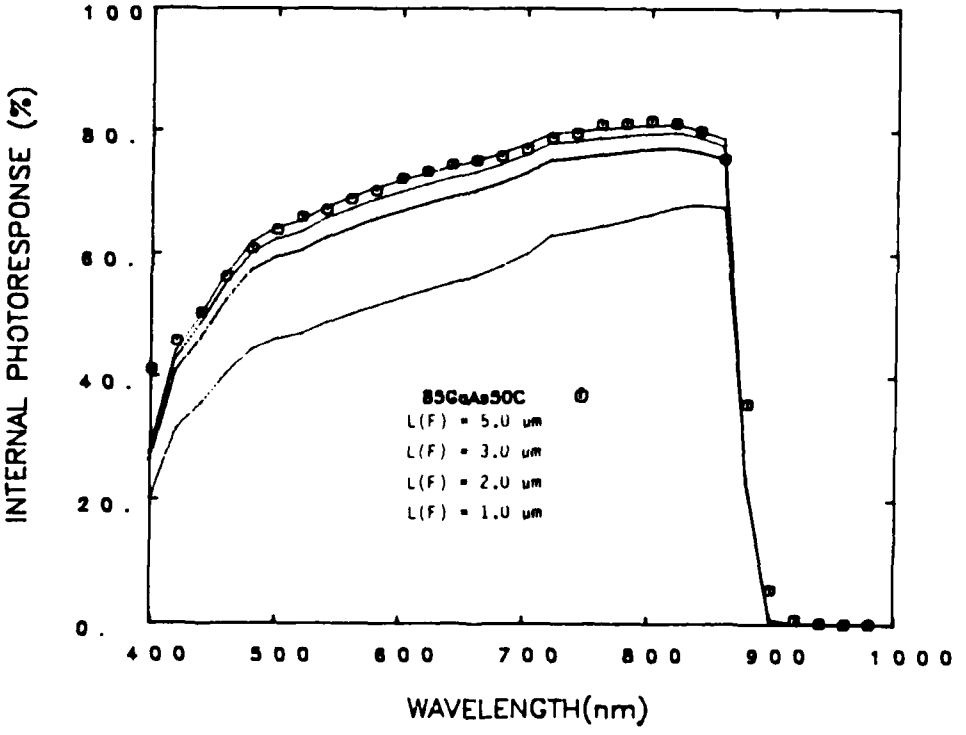

Figure 9. Internal Photoresponse Data vs. Wavelength. The Solid Lines are Calculated Results for a Range of L(F) with S(F) = 2 x 10^5 cm/sec.

We typically find L(F) to be 3 to 5 μm, and S(F) in the range of 10^4 to 10^5 cm/sec. The devices under study are emitter dominated cells. As a result, the internal photoresponse is rather insensitive to the base diffusion length. Two particularly interesting results have been obtained, namely: a light biasing effect; and the apparent existence of a 'dead layer' in the p-GaAs region, adjacent to the AlGaAs layer.

Experimental results for internal photoresponse of a typical GaAs cell are given in Figure 9 along with calculated curves for various values of L(F) and with S(F) = 2 x 10^4 cm/sec. Figure 10 illustrates the effect of varying S(F), while L(F) = 5.0 μm. The internal photoresponse of this cell is understood fairly well by setting L(F) = 5 μm and S(F) = 2 x 10^5 cm/sec. However, in order to fit the data well one must assume the existence of a dead layer on the GaAs emitter adjacent to the AlGaAs heteroface.

Figure 11 describes calculated internal photoresponse curves assuming S(F) = 2 x 10^5, L(F) = 5 μm, and four thicknesses for the 'dead layer'. Referring to Figure 12, layer 2A is the so-called dead layer. It is assumed that this region of GaAs is characterized by a negligible minority carrier lifetime. As indicated in Figure 11, it is found that the experimental curve for the internal photoresponse can only be fit by selecting a finite value for the dead layer thickness. We interpret this result as indicating that the transition region between GaAs and AlGaAs is very defective. This conclusion is supported by depth concentration profiles obtained by Auger spectroscopy.

Cells have been fabricated with the AlGaAs window layer being on the order of 300 Å thick or 500 Å. We find that devices with the thinner window layers exhibit anomalous photoresponse characteristics after an AR layer of SiN_x is deposited. The internal photoresponse is plotted for a cell under dark and light biased conditions in Figure 13. Under dark conditions, the surface recombination velocity is on the order of 10^6 cm/sec. When the cell is illuminated with approximately AM1 illumination, the internal photoresponse indicates S(F) = 10^4 cm/sec. Prior to silicon-nitride deposition, the value of S(F) is typically in the range of 10^4 to 10^5 cm/sec, and is the same under both dark and illuminated conditions.

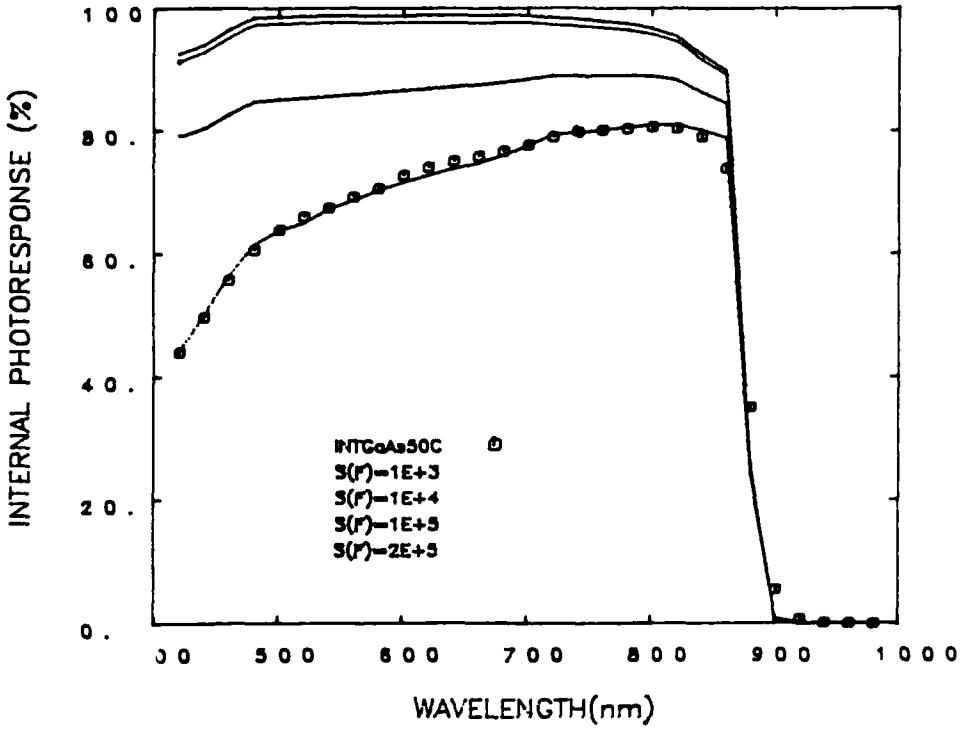

Figure 10. Calculated Photoresponse Curves with S(F) Varied and L(F) = 5.0 μm.

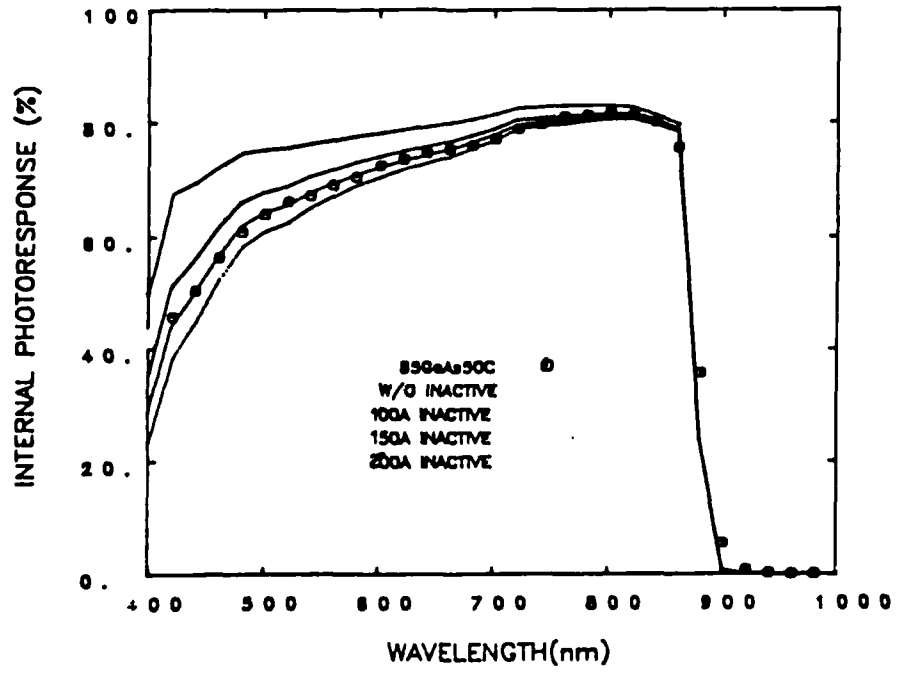

Figure 11. Calculated Photoresponse Curves with the 'Dead Layer' Thickness Varied and S(F) = 2 x 10^5 cm/sec.

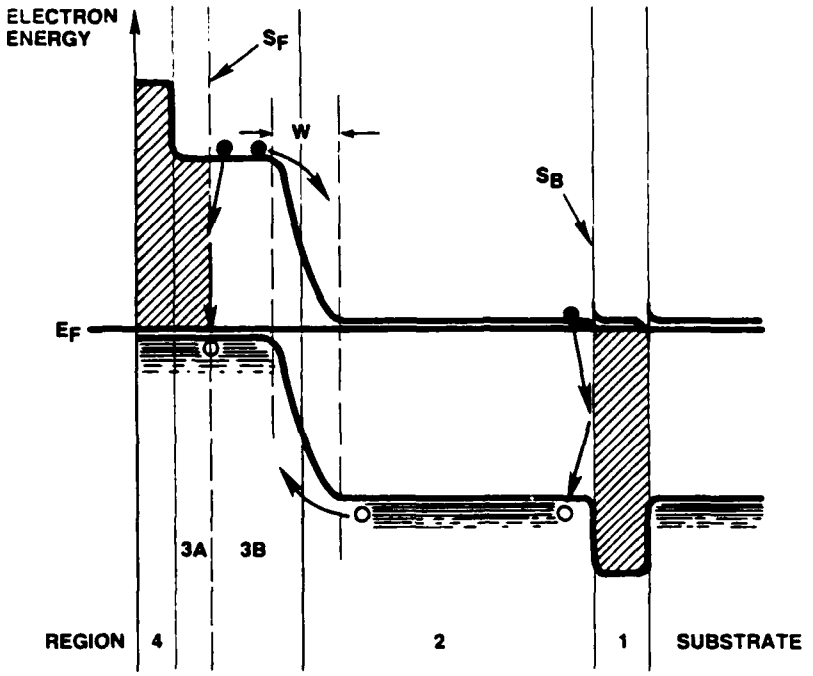

Figure 12. Electron Band Diagram for GaAs P/N Solar Cell. Layer 3A is the Proposed 'Dead Layer'.

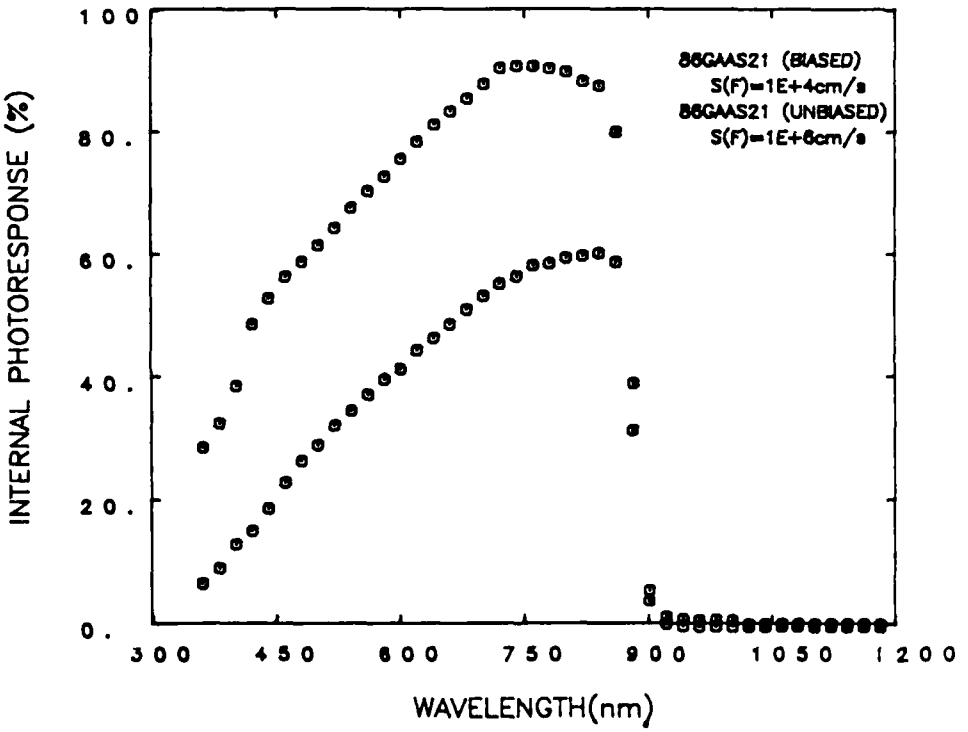

Figure 13. Internal Photoresponse of GaAs Cell Exhibiting Light Biasing Effect.

Depth concentration profiles taken by Auger spectroscopy indicate that a significant level of oxygen exists at the SiN_x-AlGaAs interface after silicon-nitride deposition. A possible explanation for the light biasing effect is that excess oxygen exists at the GaAs-AlGaAs interface giving rise to recombination centers that saturate when cells are subjected to AM1 illumination. We are not aware of any other reports of this light biasing effect in GaAs cells.

3.3 Current Loss Mechanisms

Current-voltage analyses have been carried out at various temperatures between 250°K and 400°K. Data are taken under dark and illuminated conditions. A computer based data acquisition system is utilized to obtain data points as desired at each temperature. Data are then interpreted in terms of theory. We find that I vs. V under dark conditions and I_{LOSS} vs. V (where $I_{LOSS} = I_{PH} - I$) under illuminated conditions can be interpreted in terms of two current mechanisms acting in parallel, one dominant at low voltages and one dominant at high voltages.

Thus, the current voltage characteristics can be understood in terms of two current mechanisms acting in parallel, namely,

$$I = I_1 + I_2$$

with dominant I_1 at low voltages and I_2 dominant at larger voltages. I_2 can always be written as

$$I_2 = I_{o2} \exp\left(\frac{V}{n_2 kT}\right)$$

where n_2 is independent of temperature and will vary between 1 and 2. Fitting data at various temperatures allows one to write

$$I_{o2} = I_{oo}^{(2)} \exp\left(\frac{-\phi_2}{kT}\right)$$

If the large voltage mechanism is due to minority carrier injection, $n_2 = 1.0$ and $\phi_2 = E_g$. If the dominant mechanism is due to space charge recombination, $1 < n < 2$, and $E_g/2 < \phi_2 < E_g$. The value of ϕ_2 would be related to the trap location in the latter case.

The lower voltage mechanism can usually be understood in the following manner:

$$I_1 = \begin{cases} I_{ot} \exp (BV) \\ \text{or} \\ I_{o1} \exp \left(\dfrac{V}{n_1 kT}\right) \end{cases}$$

where $I_{ot} \exp (BV)$ describes multiple step tunneling and the expression involving I_{o1} describes space charge recombination. B and n_1 are temperature independent. Thus, temperature dependent I-V analyses can lead to the identification of the dominant current loss mechanisms. As for I_{o2}, one can express I_{o1} and I_{ot} as

$$I_{ot} = I_{oo}^{(t)} \exp \left(\frac{-\phi t}{kT}\right)$$

and

$$I_{o1} = I_{oo}^{(2)} \exp \left(\frac{-\phi 1}{kT}\right)$$

ϕ_1 will be $E_g/2 < \phi_1 < E_g$, while $\phi_t \simeq 0.1$ to 0.5 eV.

Figure 14 describes typical results for the loss current vs. voltage measured under illuminated conditions. The two mechanisms are apparent. The low voltage mechanism can usually be interpreted as involving multiple-step tunneling. The upper mechanism is due to minority carrier injection or space charge recombination. In cases for which the high voltage mechanism is due to minority carrier injection, n = 1.00 and $J_o \simeq 3 \times 10^{-19}$ A/cm^2. When space charge recombination is dominant, n takes on values between 1.0 and 2.0, indicating that a wide range of recombination levels may be active in the junction region. These investigations suggest that the device edges are the sources of loss currents due to multiple-step tunneling, as well as loss currents resulting from space charge recombination.

3.4 Physical Characterization

Depth concentration profiles for the same device for which internal photoresponse data is described in Figures 9, 10 and 11 are depicted in Figure 15. The GaAs-AlGaAs transition region appears to be on the order of

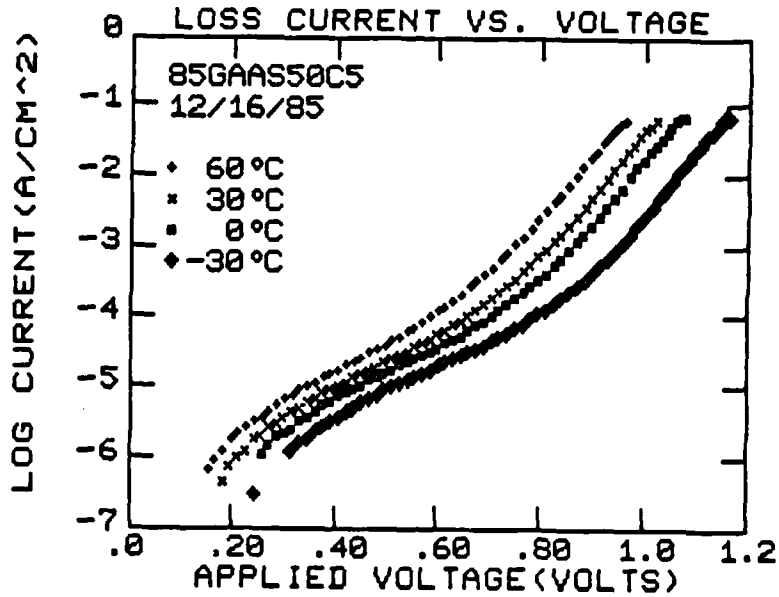

Figure 14. T-I-V Data for GaAs Cell.

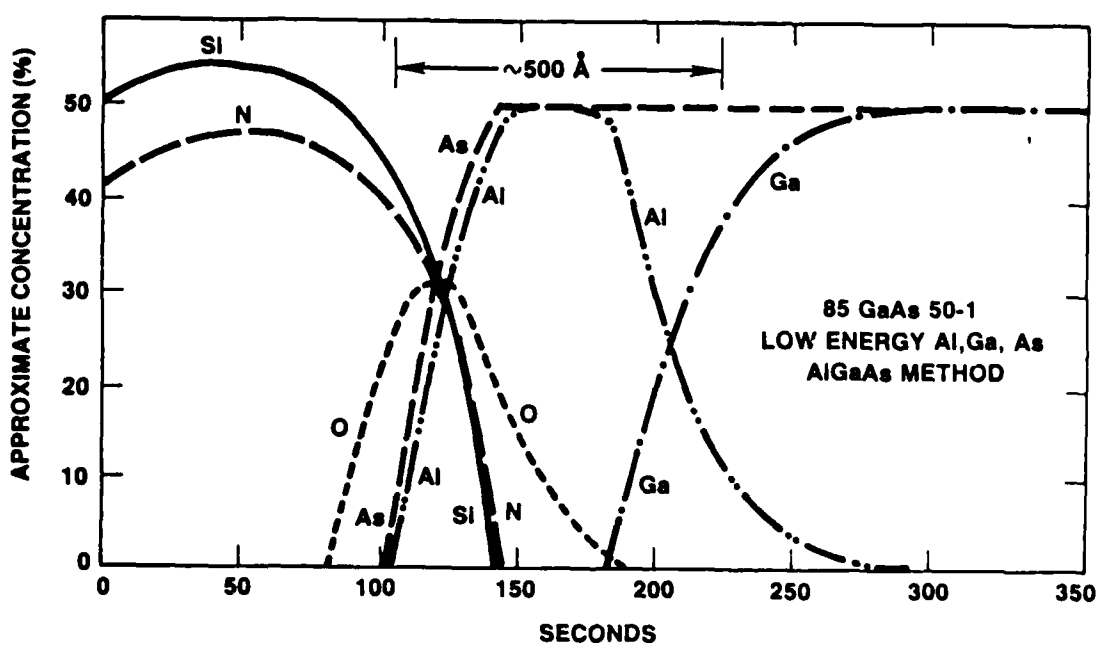

Figure 15. Depth Concentration Profiles through Heteroface Region.

400 A wide. Furthermore, as noted above, a relatively high concentration level of oxygen exists in the top layers of the device. In particular, these results suggest that a relatively high level of oxygen may exist in the GaAs-AlGaAs transition region. It is proposed that the wide transition region and oxygen impurity level may be responsible for both the light biasing effect and the dead layer.

4. KEY RESULTS AND FUTURE WORK

Significant results were obtained during FY86. Graded emitter structures were fabricated that involved a bandgap change in the emitter from 2.10 eV to 1.74. The bandgap grading results in an effective electric field of 220 V/cm. An enhanced photoresponse was observed for graded emitter devices relative to homojunction cells. Further studies were also made of GaAs solar cells to increase our baseline knowledge of III-V compound devices. Cells were fabricated with efficiencies greater than 17%.

Future work will emphasize further studies of graded emitter heterojunctions. Additional multilayer structures will be purchased from industry. It is expected that AlGaAs solar cells with graded emitters will be fabricated with efficiencies greater than 15%. These structures will provide the basis for investigating cell structures with larger graded bandgap regions. It should also be noted that AlGaAs cells are of interest for the high bandgap cell in two-cell photovoltaic systems. Furthermore, the graded emitter structure is inherently a radiation harden device structure.

A MOCVD system will be installed at the University Center by summer 1987. This system will allow us to utilize the results of device characterization to influence procedures for device fabrication in a more timely and efficient manner.

Appendix A

CONTRIBUTORS TO THE PROGRAM

Dr. Larry C. Olsen - Principal Investigator. Professor of Materials Science and Engineering. Leads program and contributes to all aspects of effort.

Dr. F. W. Addis - Research Scientist. Key person in device fabrication and solar cell characterization.

Glen Dunham - Research Engineer. Contributes to device fabrication and cell measurements.

Dan Huber - Graduate Student in Materials Science and Engineering.

Dave Daling - Graduate Student in Materials Science and Engineering.

Appendix B

STUDENT DEGREES AND THESES

Eric Eichelberger, M.S. Materials Science and Engineering, February 1986. M.S. Thesis Title: "Investigation of Solar Cells Based on MOCVD Multilayer AlGaAs Structures."

Appendix C

PUBLICATIONS AND COUPLING ACTIVITIES

Publications

"Electro-Optical Characterization of GaAs Solar Cells," Proceedings of the Space Photovoltaic Research and Technology meeting held at NASA Lewis Research Center, Cleveland, Ohio, 7-9 October 1986.

"Photoresponse Studies of GaAs Solar Cells", accepted for presentation at the 19th IEEE Photovoltaic Specialists Conference, New Orleans, Louisiana, 4-8 May 1987.

"Current Loss Mechanisms in GaAs Solar Cells", in preparation for submittal to the Journal of Electronic Materials.

Coupling Activities

"Current Loss Mechanisms in GaAs Solar Cells", presented to workshop on High Efficiency Cells at the Solar Energy Research Institute, Golden, Colorado, October 1985.

Appendix D

STATUS OF NEW MOCVD SYSTEM

An award of $278,116 was received for FY87 from DoD for the purchase of a metal organic chemical vapor deposition (MOCVD) system. The film growth system will be installed during the summer of 1987. The equipment will allow us to grow devices based on AlGaAs and InGaAsP compounds. In particular, it will be possible to grow graded bandgap structures. One feature of the system important to this program is the availability of computer control for grading film compostion.

END

5-87

DTIC